A Simple Model and Experiments for Adsorption-Desorption Hysteresis: Water Vapor on Silica Gel

Pavol Rajniak and Ralph T. Yang
Dept. of Chemical Engineering, State University of New York at Buffalo, Buffalo, NY 14260

A simple model is proposed for the evaluation of the primary and secondary adsorption and desorption processes for hysteresis-dependent sorption systems. The model is based on the use of pore blocking interpretation of hysteresis in an interconnected network of pores. The model is simple to use and requires only the primary adsorption and primary desorption isotherms to predict all secondary desorption and adsorption isotherms. A complete set of equilibrium adsorption-desorption curves covering the hysteresis loop (appearing in the range of relative pressure 0.3–0.7) was measured for water vapor on silica gel at 25°C. The usefulness of the model is supported by its agreement with experimental data.

Introduction

Adsorption is used increasingly in separation and purification processes. These processes are either transient or cyclic in which the sorbents are regenerated by desorption. For gas-phase applications, the pressure swing adsorption (PSA) process has become a major unit operation in the chemical process industry (Yang, 1987). During desorption, as the relative vapor pressure is reduced, systems in which capillary condensation occurs in the sorbents often show hysteresis, in that at some particular relative vapor pressure more gas remains adsorbed during desorption than was adsorbed during the initial adsorption process. Although hysteresis is a pervasive phenomenon, it has not been considered in the literature in the modeling and design of cyclic adsorption-desorption processes. It, however, has been considered in the study of once-through fixed-bed desorption by Ritter and Yang (1991) where significant effects caused by hysteresis were shown in the bed dynamics. This study is intended as the first effort to incorporate hysteresis into the modeling of cyclic fixed-bed adsorption-desorption processes.

The best known system in which hysteresis occurs is silica gel-water vapor. Silica gel is the most important sorbent for drying of air and industrial gases. It exhibits considerable hysteresis with many adsorbates including water vapor. Van Bemmelen first reported hysteresis in the adsorption of water on silica gel almost 100 years ago (Van Bemmelen, 1897). An excellent review of the experimental data on hysteresis, particularly on the water-silica gel system, is given by Gregg and Sing (1982). For various silica gels prepared under different conditions, the hysteresis effects are similar for water sorption (Rao, 1939; Sing and Madeley, 1954; Mikhail and Schebl, 1970; Baker and Sing, 1976; Nonaka and Ishizaki, 1977; Naono et al., 1980; Someshwar and Peshori, 1987).

Many experimental and theoretical studies have been reported on the hysteresis phenomenon (Rao, 1941; Katz, 1949; Barrer et al., 1956; Everett, 1967; Everett and Haynes, 1972; Neimark, 1986; Burgess et al., 1989; Pan and Mersmann, 1990; Rudisill et al., 1992). Of particular interest to this study are the treatments using statistical mechanical and computational techniques (Wall and Brown, 1981; Zhdanov et al., 1987; Seaton, 1991; Liu et al., 1993; Yanuka, 1990; and the literature cited therein).

The models which treat the pore system in the sorbent as an interconnected network and attribute hysteresis to pore blocking seem to give a reasonable account of most observed characteristics in hysteresis (Mason, 1982, 1983, 1988; Parlar and Yortsos, 1988, 1989). These models explain the general form of the isotherm by the concept of "pore blocking," where the emptying of a large pore filled with capillary condensed liquid is determined by the emptying of its smaller neighbors. Interpretation of these models requires a considerable amount of accurate adsorption-desorption data. In particular, accurate data within the hysteresis loop are necessary, which are scarce in the literature and are rarely complete and accurate, for the reason that often a long time (hours) is required to reach each

Correspondence concerning this article should be addressed to R. T. Yang.
Present address of P. Rajniak: Department of Chemical Engineering, Slovak Technical University, 812 37 Bratislava, Czechoslovakia.

equilibrium data point in the hysteresis loop. No complete data have been reported on the water-silica gel system.

The primary objective of this study was to provide a complete set of accurate data within the hysteresis loop for the important system of water vapor/silica gel. The second objective was to establish a simple theoretical framework for predicting the equilibrium isotherms within the hysteresis loop.

Theoretical Considerations

The theoretical basis for this study was provided by recent work of Mason (1988) and Parlar and Yortsos (1988, 1989). We consider the adsorption-desorption processes in a porous adsorbent. During the primary adsorption, the porous adsorbent initially free of the adsorbate is exposed to a vapor phase at a low pressure P. Initially the vapor molecules adsorb at particular sites on the surface of the pores and eventually form a monolayer. As the pressure is increased, multilayer adsorption occurs on the pore walls, with the adsorbed layer becoming thicker. When the condensation pressure is reached and the multilayer becomes sufficiently thick, the pore fills with the liquid-like phase. This phase transition is known as capillary condensation and commences in the finest pores at the point $L=\{x^L, a^L\}$, the lower limiting point of the hysteresis loop, as shown in Figure 1. As the pressure is progressively increased, wider and wider pores are filled until the saturation pressure is reached, where $x=1$. If the point $U=\{x^U, a^U\}$, that is, the upper limiting point of the hysteresis loop lies below the saturation pressure of the adsorbate vapor, then it is presumed that the solid has no pores of radii greater than that corresponding to the closure point. Adsorption beyond this pressure will be associated with the change of curvature of menisci freely accessible to the vapor. The corresponding equilibrium curve is termed primary (boundary) adsorption isotherm.

The primary desorption process is the reversal of the above and commences upon completion of primary adsorption at relative pressure $x=1$. The corresponding equilibrium curve is termed primary (boundary) desorption isotherm. A characteristic feature of desorption for various sorption systems is its hysteresis loop, when the adsorbed amount between points L and U is greater at any given relative pressure x along the primary desorption curve than along the primary adsorption curve. This primary desorption loop is reproducible if the desorption process commences from any point beyond the upper limiting point U or at least from this point U: $x \geq x^U$.

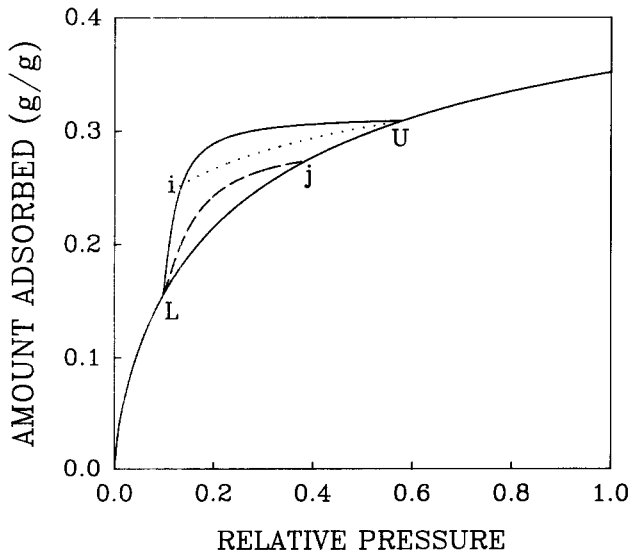

Figure 1. Adsorption-desorption hysteresis.

L and U are closure points; i and j are the starting points for secondary processes; - - - -, primary adsorption; • • • •, secondary adsorption.

Secondary (scanning) adsorption process starts from any point $i=\{x_i, a_{Di}\}$ on the primary desorption isotherm between points L and U: $x^L < x_i < x^U$. The secondary adsorption curve starting from point i will terminate at the upper limiting point of the hysteresis loop, U.

Similarly, the secondary (scanning) desorption process starts from any point $j=\{x_j, a_{Aj}\}$ on the primary adsorption isotherm between points L and U: $x^L < x_j < x^U$. The secondary desorption curve will join both boundary adsorption and boundary desorption curves at their intersection, point L.

In early studies (Rao, 1941; Katz, 1949), another kind of experimental secondary curves was reported. These curves cross over the boundary curves before joining their respective limiting point U or L. Neimark (1991) has explained the shape of two different kinds of scanning curves by the existence of two particular pore space models. The network of cavities and constrictions would result in the scanning curves shown in Figure 1. On the other hand, for the network of channels the scanning isotherms form closed loops inside the main hysteresis loop. Experimental data in this work and by A. J. Brown in 1963 (Everett, 1967; Mason, 1988), as well as recent theoretical work (Mason, 1988; Parlar and Yortsos, 1988; Ball and Evans, 1989), support only the existence of secondary sorption curves shown in Figure 1, and only these will be considered in this work. From these results it seems that the same mathematical function (isotherm) can be used to describe the primary and secondary desorption curves, which will be the first assumption in this work. A simple physical reason for the same mathematical form of the isotherm to be followed by primary and secondary desorption is that both processes undergo the same pore emptying process.

Higher-order scanning curves can also be obtained experimentally (Everett, 1967), but these are not analyzed in this work.

Following the "pore blocking" theory of Mason, a porous material (adsorbent) consists of a number of pores connected in a network. This network consists of bonds (pore throats and windows) and sites (pore bodies and cavities). The individual sites are connected via bonds. Three parameters or functions characterize the pore space: the connectivity C, the bond and site size distribution functions, $f(r)$ and $g(r)$, respectively. Connectivity is defined as the average number of bonds per pore. The characteristic dimension of the bond or the site, r, is related to the filling pressure (for capillary condensation). In Mason's treatment, the relative vapor pressure x is related to r via the macroscopic Kelvin equation for capillary condensation:

$$r = -\frac{2\sigma(T)V_L(T)}{RT \ln (P/P_o)} \tag{1}$$

where σ is the interfacial tension between liquid and gas, V_L the molar volume of the liquid adsorbate, both being function

of T, T the absolute temperature, P the vapor pressure, and P_o the saturation vapor pressure. Thus, at any value of relative pressure $x=P/P_o$, the process may be parametrized uniquely by a radius r via Eq. 1. Accordingly, the adsorption or desorption process corresponds to an increase or a decrease in r, respectively. It is worth noting that the geometric radius of a pore will be the sum of the Kelvin radius and the thickness of the adsorbed layer at the pore surface, and that the generally recognized validity for the Kelvin equation is limited to the mesopore size in the range 1 nm$<r<$25 nm.

The distribution functions $f(r)$ and $g(r)$ are normalized functions, such that $g(r)dr$ denotes the probability that a pore has a site (cavity) radius between r and $r+dr$, and similarly $f(r)dr$ is the probability of any bond (window) having a radius between r and $r+dr$. The fraction of bonds for which $r<r_p$ and so represents the probability that a capillary meniscus will not pass through a window is given by:

$$p=\int_o^{r_p} f(r)dr \tag{2}$$

and the probability that the site or the pore will be filled at the value of r_q set by P/P_o is:

$$q=\int_o^{r_q} g(r)dr \tag{3}$$

It should be noted that Mason's pore blocking theory was developed for the hysteresis (capillary condensation) domain, and therefore it describes the adsorption-desorption processes only within the range of relative pressure $x^L\le x\le x^U$. It follows then $q=p=0$ for $x=x^L$, and $q=p=1$ for $x=x^U$. The advantage of the probabilities p and q is that they make the derived functions independent of any particular pore-size distributions and the analysis is thus general; the details of the size distributions and geometry are all incorporated into the probabilities p and q.

The adsorption process in the hysteresis domain is represented by the increase of q from 0 to 1 and desorption process by the decrease of p from 1 to 0. The probabilities p and q are related through connectivity C using the inequality condition given by Mason (1989):

$$q\le p^C \tag{4}$$

The above relationship was derived from the condition that a site has its radius greater than or equal to the radius of its bonds. In fact, it may be shown (Parlar and Yortsos, 1989) that the additional constraint,

$$(1-q)^2\ge(1-p), \tag{5}$$

derived from the condition that the size of a bond is smaller than its two adjacent sites must also be satisfied. Only the limiting case of the relationship (Eq. 4),

$$q=p^C, \tag{6}$$

which considerably simplifies calculations will be used in our analysis, as has also been used by others (Mason, 1988; Ball and Evans, 1989; Parlar and Yortsos, 1988). The inequality (Eq. 4) is reduced to Eq. 6, if the radius of the site equals that of the largest bond. Any individual pore will empty at the same relative pressure at which it fills. All the hysteresis shown by systems of such pores will thus result from pore-blocking effects.

For the description of primary and secondary sorption isotherms two general variables, a and S, must be introduced. The variable a expresses the total measured amounts of adsorption or desorption (the sum of both surface adsorption and capillary condensation) in the whole range of relative pressures $0\le x\le 1$, whereas the variable S represents the fraction of pores that are filled by capillary condensation. Mason assumed that there is no correlation between the cavity radius for filling and the cavity volume. This assumption enables the number fraction to become the volume fraction. Following Parlar and Yortsos (1988), we also expect that the capillary condensation phenomenon dominates the sorption processes in the range of relative pressure $x^L<x<x^U$ and exclude secondary issues of surface adsorption in this domain. Specifically, the assumption of the dominating role of capillary condensation in the hysteresis domain requires that the contribution from surface adsorption to the total amount is constant in the range $x^L<x<x^U$ and is equal to a^L. It has been shown by Mason (1988) that for the system xenon on Vycor glass the above assumption is indeed a valid one (Figure 23 in Mason). Further justification for this assumption for the system water vapor-silica gel will be given in the section on Results and Discussion. Then, the fraction of pores filled, S, is related to adsorbed amount via the following expression:

$$S=\frac{a-a^L}{a^U-a^L} \text{ for } x^L\le x\le x^U \tag{7}$$

For the primary adsorption process (the subscript A is used for primary adsorption), the fraction of pores filled by capillary condensation is

$$S_A=q \text{ for } x^L\le x\le x^U \tag{8}$$

where q is the probability of a pore (site) being filled. It is noteworthy that neither S_A nor a_A depends on connectivity C. On adsorption the network behaves as an assembly of independent pores, and pore blocking does not play any role.

For the primary desorption the hysteresis of capillary condensed vapor can be explained by pore blocking effects, where a pore cannot empty until at least one of its neighbors has emptied. This effect depends in principle on the interconnections and the interconnectedness of the pore network. The pore structure model frequently used for the interconnectedness is the Bethe tree (Mason, 1988; Parlar and Yortsos, 1988), which has an advantage in that the description of its behavior can be expressed analytically. Alternative model structures are two-dimensional (Parlar and Yortsos, 1988) and three-dimensional crystal lattices (Seaton, 1991). The sorption hysteresis is a connectivity-related phenomenon. Such phenomena are naturally described by percolation theory (Broadbent and Hammersley, 1957). The analysis given here follows those of Mason (1988) and Parlar and Yortsos (1988) using percolation theory restricted to a Bethe tree network. Despite the fact that

the Bethe tree has no reconnections, the general forms of the percolation-related properties derived from the Bethe tree and crystal structures (with reconnections) have surprising similarities. The numerical values for thresholds, for example, differ, but the general behaviors are very similar. In particular, for desorption it is only the accessibility of the pores that is important, consequently the behavior of the Bethe tree closely follows that of lattice structures (Mason, 1988). Moreover, Mason (1982) also showed that it makes little difference which structure model is used for the range of connectivity values between 2.5 and 3.5.

During the primary desorption process, whether a site remains full or empty depends on whether one of its bonds is connected to the vapor and at the same time can also allow a capillary meniscus to pass. At some stage during primary desorption, at some value of p, the probability that a bond into a site is connected to the vapor is v. The fraction of pores filled during primary desorption, S_D (the subscript D is for primary desorption), at corresponding values of probabilities p and v, is shown by Mason (1988) as:

$$S_D = (1 - v)^{C/(C-1)} \tag{9}$$

$$p = (S_D^{1/C} - S_D^{(C-1)/C})/(1 - S_D^{(C-1)/C}) \tag{10}$$

Equations 9 and 10 yield the following limiting values: $S_D = 1$ for $v = 0$ and $S_D = p = 0$ for $v = 1$. Plots of S_D against p for various values of C have been given by Mason (1988).

For the secondary adsorption process (the subscript SA is for secondary adsorption) starting from any point i on the boundary desorption curve (see Figure 1), the following simple expression was derived (Mason, 1988; Parlar and Yortsos, 1988):

$$\frac{a_{\max} - a_{SA}}{a_{\max} - a_A} = \frac{1 - S_i}{1 - q_i} \tag{11}$$

where S_i is the fraction of pores filled at point i, and q_i is the corresponding probability in which a site is filled at partial pressure x_i. The variables a_A and a_{SA} represent adsorbed amounts on the primary adsorption isotherm and the secondary adsorption isotherm, respectively, at any point within $x_i < x < x^U$.

In an earlier analysis, Mason (1983) used the assumption that $a_{\max} = a^U$ for the whole adsorption scanning curve. In a more recent work (Mason, 1988), he proposed to compute $a_{\max}$ by an empirical equation. For the general case $x^U \neq 1$, this equation is given as:

$$a_{\max} = a^U - \kappa \ln (x^U/x) \text{ for } x \leq x^U \tag{12}$$

where κ is an empirical constant evaluated from experiments.

From Eq. 11 it follows that the secondary adsorption curves join the boundary adsorption curve at the upper closure point of hysteresis loop U, where $a_{SA} = a_A = a_{\max} = a_D = a^U$. For the case $a^U = a_{\max}$, Eq. 11 can be written, using Eqs. 7 and 8, as follows:

$$\frac{a^U - a_{SA}}{a^U - a_A} = \frac{a^U - a_{Di}}{a^U - a_{Ai}} \tag{13}$$

The analysis for the secondary desorption process is a more complicated problem. Pore blocking during desorption is controlled by the pore space connectivity and the bond radius distribution. For the secondary desorption process starting from point j on the boundary adsorption isotherm (see Figure 1), Mason (1988) derived the following relationships:

$$p = \frac{q_j^{1/C}[(1-u)^{1/C} - q_j(1-u)]}{1 - q_j(1-u)} \tag{14}$$

$$\frac{1 - S_{SD}}{1 - S_A} = \frac{1 - q_j(1-u)^{C/(C-1)}}{1 - p^C} \tag{15}$$

where q_j is the corresponding probability at point j and is simply equal to S_j (see Eq. 8). Note that Eqs. 9 and 10 follow directly from Eqs. 14 and 15 by taking $q_j = 1$. The probability p and the fraction of pores filled S_{SD} at any point on the secondary desorption curve in the range $x^L < x < x_j$ are related to the variable u, which gives the probability that at a particular value of p an initially filled bond into a site now has an emptied neighbor and so has a connection to the vapor. It is worth noting that in the beginning of secondary desorption, for $x = x_j$, $u = 0$. Equations 14 and 15 are rather involved: to relate them to a particular partial pressure (x) during secondary desorption, both bond size distribution $f(r)$ and connectivity C have to be known. Useful simplifications, however, may be obtained near point j, the starting point of the jth secondary desorption isotherm.

Parlar and Yortsos (1988) developed a percolation model for hysteresis-dependent sorption phenomena and extended Mason's (1983) previous work. In contrast to Mason's model, Parlar and Yortsos assume a correlation between the site volume and the site radius. Thus, both pore-size and pore-volume distributions are incorporated in their model. For the Bethe lattice they derived expressions that are in agreement with adsorption as well as primary desorption. The expressions for secondary desorption curves, however, are different between the two models. At the onset of secondary desorption (point j), Parlar and Yortsos (1988) derived for the ratio between the slopes of the jth secondary desorption and the primary adsorption isotherms the following relationship:

$$\frac{(dS_{SD}^t/dx)_{x=x_j}}{(dS_A^t/dx)_{x=x_j}} = 1 - q_j^{(C-1)/C} \tag{16}$$

where the superscript t stands for theoretical. In contrast, from Mason's results, Eqs. 6, 14 and 15, which are based on a network of constant-volume sites, we get after several manipulations the different expression:

$$\frac{(dS_{SD}^t/dx)_{x=x_j}}{(dS_A^t/dx)_{x=x_j}} = 1 - q_j \tag{17}$$

The probability q_j is identical to the fraction of pores filled, S_j, which can be obtained from experimental data (see Eqs. 7 and 8). Neither connectivity C nor size distribution functions are needed for Eq. 17. The two different results are caused by the different assumption used in the two models, as mentioned above. Equation 17 will be used in this work.

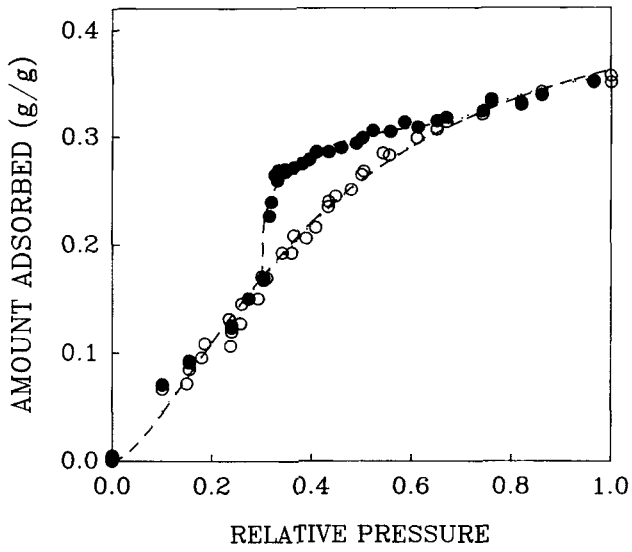

Figure 2. Equilibrium data for water vapor on silica gel at 25°C.

o, primary adsorption; •, primary desorption. All primary data are from Table 1. Data fitting by the LF isotherm (- - - -) and *DA* isotherm (• • • •).

Equation 17 can be rewritten using the fraction S defined in Eq. 7 as follows:

$$\frac{(da'_{SD}/dx)_{x=x_j}}{(da'_A/dx)_{x=x_j}} = 1 - q_j \tag{18}$$

For the primary desorption curve, $q_j = 1$, we get:

$$\frac{(da'_D/dx)_{x=x_j}}{(da'_A/dx)_{x=x_j}} = 0 \tag{19}$$

The theoretical conditions (Eqs. 18 and 19) are not completely fulfilled for real experimental data (the superscript r stands for real), which is apparent from the shape of experimental primary desorption isotherm, shown in Figure 2. At the onset of primary desorption we have $a'_D \neq a'_D = a^{\mu}$ and consequently $(da'_D/dx)_{x=x^{\mu}} > 0$. The nonhorizontal linearity of the desorption isotherm in this region can be explained by the decompression of the liquid phase (Mason, 1988; Seaton, 1991). In the more recent work of Seaton and coworkers (Liu et al., 1992), however, it was noted that decompression of the liquid phase was not sufficient to describe desorption in this region, and the vaporization via surface clusters of vapor-filled pores was taken into account. On the other hand, Parlar and Yortsos (1989) showed that the deviations from a theoretical (percolation) behavior could likewise be explained by nucleation. As nucleation, vaporization from surface clusters and decompression of the liquid phase all yield almost linear desorption isotherms near the upper closure point; therefore, it is difficult to separate the three effects. We have proposed to express these "dispersion" effects in the whole hysteresis domain by the following empirical expression, which is analogous to the correction, Eq. 12, proposed by Mason for the maximum amount adsorbed:

$$a^r = a^t - \kappa \ln (x^{\mu}/x) \tag{20}$$

and assume $a_{max} = a^U$ for the whole hysteresis domain.

For the derivative of the primary desorption isotherm at the onset of desorption (or near point U or before the percolation threshold), we get:

$$(da'_D/dx) = (da^t_D/dx) + \kappa/x = \kappa/x \tag{21}$$

Consequently, the theoretical condition (Eq. 19) can be rewritten for real experimental data as follows:

$$\frac{(da'_D/dx)_{x=x^{\mu}}}{(da'_A/dx)_{x=x^{\mu}}} = \frac{\kappa/x^{\mu}}{(da'_A/dx)_{x=x^{\mu}}} \tag{22}$$

The same correction procedure can be employed for the secondary desorption isotherms, and condition 18 can be rewritten:

$$\frac{(da'_{SD}/dx)_{x=x_j}}{(da'_A/dx)_{x=x_j}} = 1 - q_j + \frac{\kappa/x_j}{(da'_A/dx)_{x=x_j}} = E_j \tag{23}$$

Equation 23 expresses the first condition which must be satisfied for the jth secondary desorption isotherm starting from point j on the boundary adsorption curve. The righthand side of Eq. 23, E_j, can be evaluated from experimental data.

The second condition immediately follows for the intersection of the primary adsorption curve and the secondary desorption curve at point j (Figure 1):

$$a'_A = a'_{SD} \text{ for } x = x_j \tag{24}$$

(In the remainder of this work, we will deal with only real experimental data and the superscript r will be omitted.)

All methods cited above were originally developed for the evaluation of connectivity and pore-size distribution functions for porous materials. These methods require a significant amount of accurate experimental data for primary adsorption process and for both primary and secondary desorption processes. Secondary (scanning) adsorption curves can provide only a test of the model, because they cannot be used in pore-size distributions and connectivity evaluation. Calculation of the secondary adsorption isotherms can be readily accomplished by using Eq. 13.

Equations 14 and 15 are the basis from Mason's theory for calculating the secondary desorption isotherms. The use of these equations, however, is rather complicated and requires additional assumptions and empirical parameters. First, the value of the connectivity, C, needs to be obtained by empirical data fitting. Secondly, the partial pressure, P or $x = P/P_o$, must be related to the bond filling probability, p, through the bond (window) size distribution function, $f(r)$, Eq. 2. Here, Kelvin equation, Eq. 1, is the additional equation which relates P to r. The bond-size distribution remains an unknown function. This function cannot be determined experimentally for any real material with a random pore structure. One may assume an $f(r)$ function, such as Gaussian; then at least two more empirical parameters are needed. A large amount of computation, as well as empiricism involved in using Eqs. 14 and 15,

makes it impractical and undesirable for process simulation such as that for fixed-bed adsorber processes.

The approach taken here is a phenomenological one. As mentioned, all secondary desorption isotherms terminate at the lower closure point, L. Also, based on all available experimental data as well as physical grounds, it is reasonable to use the same mathematical function (isotherm) that is used for the primary desorption curve to describe all secondary desorption curves. The simple physical reason for this is that both primary and secondary desorption curves undergo the same pore emptying process, differing only in the starting point. (Further experimental results in this work will show that this approach is indeed a sound one.) Once the isotherm function is chosen, the isotherm parameters are fixed by fulfilling the two constraints, Eqs. 23 and 24.

Since hysteresis is a phenomenon involving pore filling (or capillary condensation), the isotherms based on pore-filling theory (or potential theory) would be more meaningful for describing the scanning curves. The numerous isotherms based on potential theory (Yang, 1987) are especially useful for adsorption on microporous materials and can describe the adsorption of vapors on porous adsorbents over a wide range of pressures up to saturation (Kapoor et al., 1989). Among them, the Dubinin-Astakhov (DA) equation,

$$V = V_o \exp\left(-\frac{A}{\beta E_o}\right)^{n_A}, \tag{25}$$

and the simpler Dubinin-Radushkevich (DR) equation, for which $n_A = 2$, are the most common. V is the volume of pores filled at relative pressure x, V_o is the limiting pore volume, $A = RT \ln (1/x)$ which is the adsorption potential or differential molar work of adsorption, β is the affinity or similarity coefficient which depends on the adsorptive, and E_o is a characteristic energy which depends on the microporous structure of the adsorbent. It has long been known that the characteristic energy, E_o, is related to the pore size, being greater for smaller pore sizes (Stoeckli, 1977). The exponent n reflects the structural heterogeneity, being large for a narrow pore-size distribution, and lies in the range 1-4. The adsorbed volume can be converted to the amount adsorbed by assuming the adsorbed phase as liquid. Then, Eq. 25 can be written for the primary adsorption as:

$$a_A = a_{mA} \exp\left[-\left(K_A \ln \frac{1}{x}\right)^{n_A}\right] \tag{26}$$

with $n_A = 2$ for the DR equation. Alternatively, the adsorption data can be described using the Langmuir-Freundlich (LF) equation, expressed in the form:

$$a_A = a_{mA} \frac{K_A x_A^n}{1 + K_A x^{n_A}} \tag{27}$$

which for $n_A = 1$ becomes the Langmuir (LA) equation.

The primary adsorption measurements of various authors for water on regular density silica gels were correlated using a two-site DR equation (Van den Bulck, 1990). The primary adsorption data for grade 01 Davison silica gel were fitted with a two-site LF expression (Jury and Edwards, 1971). The authors also showed that the adsorption process can be explained in terms of Polanyi's potential theory.

The hysteresis effects were first considered in modeling of fixed-bed desorption in the study of Ritter and Yang (1991), using only primary curves. For the primary desorption data of Sing and Madeley (1954), the Langmuir-type correlation was applied in the range $x^L \le x \le x^U$ (Ritter and Yang, 1991):

$$a_D = a^L + a_{mD} \frac{K_D (x - x^L)^{n_D}}{1 + K_D (x - x^L)^{n_D}} \tag{28}$$

The above equation is referred to as Langmuir-Freundlich isotherm, with $n_D = 1$ for Langmuir isotherm.

The corresponding DA equation is:

$$a_D = a^L + a_{mD} \exp\left[-\left(K_D \ln \frac{1}{(x - x^L)}\right)^{n_D}\right] \tag{29}$$

with $n_D = 2$ for the DR expression.

For the jth secondary desorption curve starting from point $\{x_j, a_{A_j}\}$ the following LF relationship corresponding to Eq. 28 may be used for the range $x^L \le x \le x_j$:

$$a_{SD} = a^L + a_{mj} \frac{K_j (x - x^L)^{n_D}}{1 + K_j (x - x^L)^{n_D}} \tag{30}$$

Similarly, the DA expression for the secondary desorption isotherms is written as:

$$a_{SD} = a^L + a_{mj} \exp\left[-\left(K_k \ln \frac{1}{(x - x^L)}\right)^{n_D}\right] \tag{31}$$

In the isotherm equation for the secondary desorption, only two parameters can be determined, because only two equations (Eqs. 23 and 24) are available from the percolation theory which the secondary desorption isotherm must satisfy. A number of two-parameter isotherms have been derived for multilayer adsorption for Type II isotherms, such as BET and Frenkel-Halsey-Hill (FHH) isotherms (Gregg and Sing, 1982). They may be used here; the FHH isotherm is particularly attractive for its simple mathematical form. For the three-parameter DA and LF equations, we choose to fix the exponent, n_D, and vary the other two parameters for secondary desorption curves starting from different points. In the DA equation, the maximum amount adsorbed a_{mj} expresses the maximum micropore volume, and the parameter K_j is correlated through E_o with the pore size. For secondary desorption processes starting at different points j on the boundary adsorption curve, the initial amount adsorbed and the size of the pores to be emptied are different. From this point of view, the assumption of different a_{mj} and K_j for various desorption isotherms seems to be theoretically acceptable. Alternatively, one may assume the same limiting pore volume, a_{mj}, and vary K_j and n_D. For the LF equation, Eq. 30, n_D is fixed for the reason that n_D has been related to the lateral interaction energy (Yang, 1987).

Based on the theoretical framework, the following is a simple, step-by-step procedure for predicting the secondary isotherms within the hysteresis loop from the primary isotherms:

Step 1. Evaluate the isotherm parameters for the primary adsorption process (a_{mA}, K_A, n_A) by nonlinear regression.

Step 2. Determine the positions of the two limiting (closure) points of the hysteresis loop, L and U (x^L, x^U).

Step 3. Evaluate the isotherm parameters for the primary desorption process (a_{mD}, K_D, n_D) by nonlinear regression. (Steps 2 and 3 can be combined in the case of uncertain position for point U, as will be described shortly.)

No other information is needed for *a priori* computation of the secondary adsorption and desorption isotherms.

For secondary adsorption starting from point i, the isotherm is evaluated by Eq. 13, which may be recast as:

$$a_{SA} = a^U\left(\frac{a_{Di}-a_{Ai}}{a^U-a_{Ai}}\right) + \left(\frac{a^U-a_{Di}}{a^U-a_{Ai}}\right)a_A \qquad (32)$$

For point $i=\{x_i, a_{Di}\}$ the adsorbed amount a_{Ai} on the boundary adsorption curve and the adsorbed amount a_A for any point x in the range $x_i<x<x^U$ can be computed using the primary adsorption isotherm, Eq. 26 or 27.

For secondary desorption starting from point j, two isotherm parameters (for example, a_{mj}, K_j in Eq. 30 or 31) are evaluated from Eqs. 23 and 24.

Experimental Studies

Adsorbent

The silica gel used in the experiments was a standard commercial desiccant, Davison Grade H Type, mesh size 28-200. Adsorption data for nitrogen at the liquid N_2 temperature, 77 K, were obtained using a Carlo Erba Sorptomatic 1900 apparatus. There was complete reversibility in the entire pressure range. The specific surface area and pore volume were determined using BET isotherm to be 767 m^2/g and 0.398 cm^3/g, respectively. The nitrogen adsorption (desorption) isotherm was nearly identical with the data reported by Mikhail et al. (1968) for microporous silica gel Davidson 03. Their specific surface area and pore volume were 793 m^2/g and 0.409 cm^3/g, respectively. They also evaluated the pore-volume distribution using the extended de Boer method and obtained the most frequent pore width to be about 0.9 nm and the maximum pore width of about 1.6 nm, showing that the gel contained only micropores. It may be noted, however, that the surface area available to water, which may differ from that to N_2 at 77 K, is relevant to this work.

Adsorption apparatus

Equilibrium data were measured using a Mettler TA2000C Thermoanalyzer (TGA). High-purity helium was used as the inert carrier gas and for regeneration. The generation of water vapor at the desired partial pressure was accomplished by bubbling He through a gas wash bottle and proportioning with a diluent He (Baksh, 1991). A sampling port located at the entrance to the TGA provided a source for checking the composition using gas chromatography.

The TGA microbalance measured weight changes of the adsorbent accurate up to 10^{-5} g. The adsorptive entered through the TGA inlet and flowed over the adsorbent before exiting. Weight changes were continually recorded.

Experimental procedure

The results of previous investigations (Lunde and Kester, 1975; Baker and Sing, 1976; Naono et al., 1980) showed that on the dehydroxylated surfaces of silica gels, true physical adsorption equilibrium was not obtained in the first adsorption run because of slow chemisorption. The slow chemisorption gives rise to low-pressure hysteresis in the water vapor isotherm. The dehydroxylated silica can be adequately rehydroxylated by water vapor at high relative pressures.

The sample of silica gel was activated by purging with high-purity helium for 2 hours at 200°C. The weight of the sample after activation was 54.02 mg.

The first adsorption run was made at 25°C up to saturation relative pressure, $P/P_o=1$. After the adsorbent had been exposed to water vapor at saturation pressure for 6 hours, the first desorption run was carried out by passing pure helium over the sample. After the first desorption, the gel retained 3.32 mg of water, which was not removable after 5 hours of purging. This amount of chemisorbed water remained unaltered in subsequent adsorption and desorptions. The weight of the rehydroxylated sample (57.34 mg) was taken as the basis for sorption data evaluation.

Successive adsorptions and desorptions were conducted at 25°C by changing the composition of the adsorptive and allowing adequate time to establish equilibrium. It was important to ensure that each point on the isotherms was measured under equilibrium conditions. To achieve this, the time required for some points was as long as 26 hours, particularly for the desorption measurements near the threshold leading to the steep desorption region.

The hysteresis loop obtained for the system was scanned by starting from various points on the primary (boundary) adsorption curve and the primary (boundary) desorption curve, thus generating a large set of secondary desorption and adsorption curves. The complete equilibrium data set is given in Table 1.

Results and Discussion

First, the assumption of the dominant role of capillary condensation in the hysteresis domain was tested by the procedure suggested by Mason (1988). The contribution by surface adsorption in the range of relative pressures $x^L<x<x^U$ was estimated (using Eq. 32 in Mason, 1988). The amount of surface adsorption increased only slightly, from $a^L=0.174$ g/g at $x=x^L$ to 0.185 g/g at $x=x^U$. This result indicates that surface adsorption is relatively constant, and capillary condensation plays a dominating role in the hysteresis domain for the system of water vapor-silica gel.

The experimental data in Table 1 exhibit well behaved and reproducible hysteresis curves in the range of relative pressures 0.3-0.7. The position and shape of the observed hysteresis loop of Type-H2 (IUPAC classification) are in good agreement with the previous experiments for this system (Sing and Madeley, 1954; Baker and Sing, 1976; Park and Knaebel, 1992).

The adsorption-desorption experimental data were analyzed with Langmuir (LA), Langmuir-Freundlich (LF), Dubinin-Astakhov (DA) and Dubinin-Radushkevich (DR) expressions.

The comparison of the fit of data by various models is based on the sum of squares, SS:

Table 1. Sequential, Equilibrium Adsorption-Desorption for Water Vapor on Silica Gel at 25°C

Point	x	a	Point	x	a	Point	x	a
1	0.000	0.000	41	0.293	0.151	81	0.489	0.269
2	0.101	0.067	42	0.341	0.193	82	0.440	0.263
3	0.155	0.091	43	0.390	0.206	83	0.401	0.233
4	0.240	0.126	44	0.434	0.235	84	0.350	0.211
5	0.310	0.170	45	0.505	0.268	85	0.313	0.180
6	0.365	0.209	46	0.543	0.285	86	0.238	0.107
7	0.435	0.240	47	0.610	0.302	87	0.000	0.001
8	0.501	0.265	48	0.589	0.299	88	0.235	0.130
9	0.556	0.283	49	0.564	0.294	89	0.360	0.193
10	0.611	0.299	50	0.540	0.293	90	0.651	0.307
11	0.670	0.314	51	0.516	0.290	91	0.743	0.321
12	0.760	0.333	52	0.482	0.283	92	0.820	0.332
13	0.861	0.342	53	0.436	0.274	93	0.998	0.351
14	0.965	0.351	54	0.426	0.273	94	0.820	0.332
15	0.997	0.357	55	0.406	0.266	95	0.743	0.324
16	0.965	0.352	56	0.376	0.259	96	0.651	0.315
17	0.861	0.339	57	0.350	0.252	97	0.586	0.314
18	0.760	0.335	58	0.319	0.191	98	0.523	0.306
19	0.670	0.318	59	0.304	0.170	99	0.410	0.286
20	0.613	0.309	60	0.240	0.120	100	0.347	0.270
21	0.558	0.305	61	0.150	0.072	101	0.334	0.269
22	0.502	0.299	62	0.000	0.005	102	0.327	0.265
23	0.490	0.294	63	0.186	0.109	103	0.316	0.227
24	0.460	0.290	64	0.480	0.251	104	0.330	0.245
25	0.435	0.286	65	0.575	0.289	105	0.356	0.252
26	0.396	0.278	66	0.548	0.285	106	0.382	0.255
27	0.381	0.275	67	0.518	0.281	107	0.470	0.273
28	0.365	0.272	68	0.484	0.272	108	0.536	0.281
29	0.348	0.268	69	0.439	0.268	109	0.606	0.297
30	0.332	0.260	70	0.390	0.252	110	0.701	0.311
31	0.320	0.240	71	0.364	0.241	111	0.961	0.350
32	0.304	0.168	72	0.358	0.240	112	0.325	0.252
33	0.274	0.151	73	0.332	0.202	113	0.341	0.259
34	0.240	0.124	74	0.300	0.171	114	0.355	0.263
35	0.155	0.093	75	0.000	0.002	115	0.383	0.270
36	0.101	0.071	76	0.260	0.146	116	0.470	0.285
37	0.000	0.003	77	0.409	0.216	117	0.565	0.301
38	0.155	0.085	78	0.449	0.245	118	0.630	0.311
39	0.180	0.096	79	0.538	0.279	119	0.711	0.319
40	0.258	0.128	80	0.523	0.275	120	0.921	0.341

$$SS = \sum_{j=1}^{N} (a_{\text{cal}} - a_{\text{exp}})_j^2 \tag{33}$$

where N is the number of data points, a_{cal} and a_{exp} are the calculated and experimental amounts adsorbed, respectively. It has been suggested (Kinnlburgh, 1986) that various isotherms with different number of parameters can be compared in terms of the residual root mean square error (RRMSE) given by:

$$\text{RRMSE} = \left(\frac{SS}{N-M}\right)^{0.5} \tag{34}$$

where M is the number of parameters of the model.

First, the parameters a_{mA}, K_A and n_A were determined for the primary adsorption isotherm by nonlinear regression. The results are given in Table 2.

In the second step, positions of both limiting (closure) points of the hysteresis loop, L and U, were specified. The uncertainties involved in determining the locations of the closure points have been discussed (Burgess et al., 1989, and the literature cited therein). For our experimental data, the location of the lower limiting point, L, can be well determined *a priori* from primary and secondary desorption curves. The value of the relative pressure $x^L = 0.3$ was taken for the subsequent analysis.

Similar *a priori* determination of the upper limiting point from experimental data is rather uncertain. The theoretical

Table 2. Sequential Regression Analysis of Primary Adsorption Data

Isotherm	a_{mA}	K_A	n_A	RRMSE	x^L
LA	0.777	0.945	1.0*	1.406×10^{-2}	0.3*
LF	0.454	3.957	1.565	0.919×10^{-2}	0.3*
DR	0.338	0.682	2.0*	1.309×10^{-2}	0.3*
DA	0.355	0.686	1.556	0.825×10^{-2}	0.3*

LA = Langmuir; *LF* = Langmuir-Freundlich; *DR* = Dubinin-Radushkevich; *DA* = Dubinin-Astakhov; * = fixed value; RRMSE = residual root-mean-square error

location corresponding to the upper limit of validity of the Kelvin equation for capillary condensation is $x^U \cong 0.95$. For our experimental system, however, the boundary adsorption and boundary desorption curves coincide (within the limit of experimental error) for relative pressures at $x > 0.7$. Consequently, it seemed reasonable to obtain the value for x^U from the intersection of the two primary isotherms.

In the third step, the parameters a_{mD}, K_D, and n_D were determined for the primary desorption isotherm with the lower limiting point at $x^L = 0.3$. The results are given in Table 3.

The location of the upper limiting point, U, was subsequently determined as the intersection of the primary adsorption and primary desorption isotherms. A simple trial-and-error procedure was employed for this purpose. The results are also given in Table 3. The values of κ were calculated from experimental data by using Eq. 21 at the upper closure point:

$$\left(\frac{da_D}{dx}\right)_{x=x^U} = \frac{\kappa}{x^U} \tag{21a}$$

These values are included in Table 3.

The results in Tables 2 and 3 show that the best agreement with experimental data was obtained with the DA-type relations, Eqs. 27 and 28, for primary adsorption and primary desorption, respectively. Only slightly less agreement was obtained with the LF-type expressions, Eqs. 26 and 29. The description for primary processes with the LA or DR relations was less satisfactory, in particular for primary adsorption at relative pressure $x > 0.7$, where the relative error exceeded 8%. Figure 2 shows the comparison between experimental data and the LF and DA equation fittings using the parameters in Tables 2 and 3.

One may predict the primary desorption isotherm from the primary adsorption isotherm using Mason's pore blocking theory, if the positions of points L and U and the value of connectivity are known. The following is a simplified procedure carried out assuming that surface adsorption is unimportant, and only capillary condensation counts for the amount adsorbed. Since the connectivity, C, is not known, it remains a fitting parameter to be determined by matching the experimental desorption data. From Mason's theory, Eqs. 9 and 10, however, the primary desorption (S_D) is calculated as a function of bond probability (p). One needs to relate p with partial pressure, x. Here, we relate p with x through the primary adsorption isotherm (a_A) as follows:

$$p^C = q = \frac{a_A - a^L}{a^U - a^L} \tag{35}$$

and a_A is related to x through the primary adsorption isotherm, Eq. 26 or 27. Equation 35 follows directly from Eqs. 6 and 7. By using this procedure, one can calculate a set of $S_D(x)$ from any given value of v, using Eqs. 9, 10, 35 and 26 (or 27). Equation 20 is the additional equation for determining the value of κ.

Figure 3 shows the results for the primary desorption calculated based on Mason's theory with adjustable parameters $C = 2.61$ and $\kappa = 0.062$ obtained by nonlinear regression. The theoretical result for $\kappa = 0$ is also shown here. These results are compared with curve fitting using the LF isotherm, Eq. 30,

Table 3. Sequential Regression Analysis of Primary Desorption Data

Isotherm	a_{mD}	K_D	n_D	RRMSE	x^U	κ^*
LA	0.142	46.76	1.0*	0.728×10^{-2}	0.690	0.012
LF	0.204	3.795	0.475	0.641×10^{-2}	0.700	0.035
DR	0.144	0.213	2.0*	0.646×10^{-2}	0.643	0.025
DA	0.157	0.205	1.534	0.640×10^{-2}	0.683	0.034

*See Table 2 for notation; κ was calculated separately (see text).

with parameters in Tables 2 and 3. Note the horizontal linearity and sharp desorption threshold on the theoretical curve. For the following analysis of the secondary processes, we will use only the LF- and DA-type isotherms.

From the primary adsorption and desorption isotherms, the secondary desorption isotherms were then predicted. Equation 23 may be expressed either by the LF or DA isotherms. Substituting Eqs. 27 and 30 into Eq. 23, one gets:

$$\frac{a_{mj}K_j n_D (x_j - x^L)^{n_D - 1}(1 + K_A x^{n_A})^2}{a_{mA}K_A n_A x^{n_A - 1}[1 + K_j(x_j - x^L)^{n_D}]^2} = E_j \tag{36}$$

where E_j is the ratio of derivatives from Eq. 23. In Eq. 23, the value of q_j can be calculated from Eqs. 7 and 8 at point j on the primary adsorption curve, and that for κ it can be taken from Eq. 21a.

Substituting Eqs. 27 and 30 into Eq. 24, we get for the intersection of the primary adsorption curve and the secondary desorption curve at point $j = \{x_j, a_{Aj}\}$ the second condition:

$$a_{mA}\frac{K_A x_j^{n_A}}{1 + K_A x_j^{n_A}} = a^L + a_{mj}\frac{K_j(x_j - x^L)^{n_D}}{1 + K_j(x_j - x^L)^{n_D}} \tag{37}$$

Combining Eqs. 36 and 37, the parameters of jth secondary desorption curve, K_j and a_{mj}, can be expressed explicitly by:

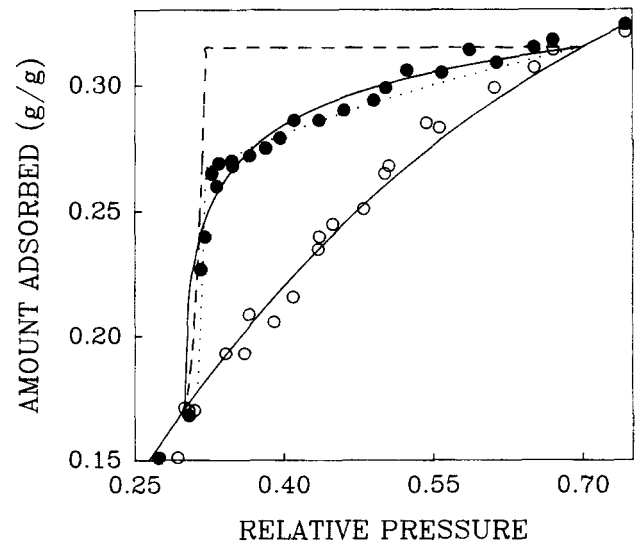

Figure 3. Primary adsorption and desorption data (from Table 1).

Fitted by the LF isotherm (——) and compared to the pore-blocking theory of Mason with $C = 2.61$ and $\kappa = 0$ (- - - -), and $C = 2.61$ and $\kappa = 0.062$ (• • • •).

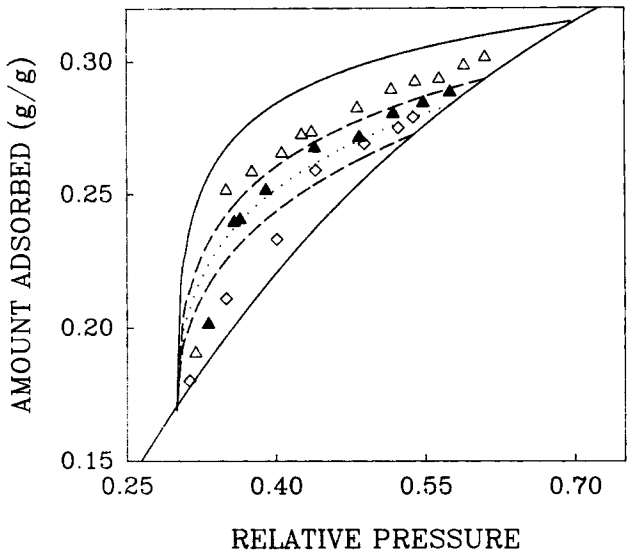

Figure 4. Experimental data (symbols) of equilibrium secondary desorption vs. proposed model (curves) from primary adsorption-desorption data using the LF isotherm.

$$K_j = \frac{A_j D_j - B_j C_j}{B_j C_j^2} \qquad a_{mj} = \frac{D_j(1 + K_j C_j)}{K_j C_j} \tag{38}$$

where

$$A_j = n_A (x_j - x^L)^{n_A - 1}(1 + K_A x_j^{n_A})^2 \qquad B_j = E_j a_{mA} K_A n_A x_j^{n_A - 1}$$

$$C_j = (x_j - x^L)^{n_D} \qquad D_j = a_{Aj} - a^L$$

Using the same procedure for the DA isotherms, we get the following expressions:

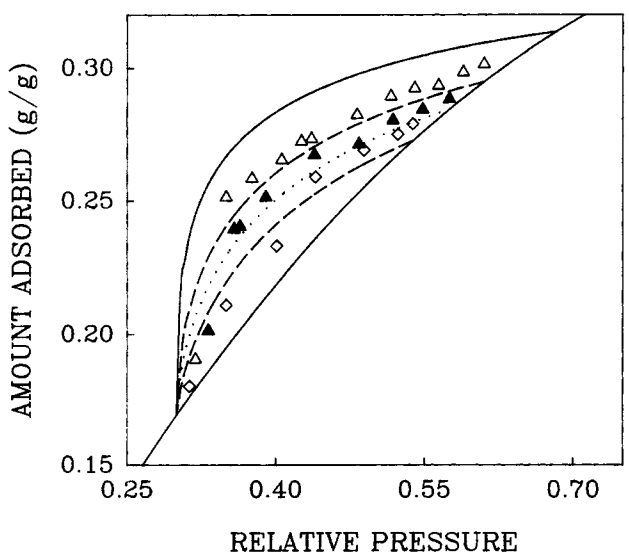

Figure 5. Same as in Figure 4, except for the DA isotherm.

Table 4. Comparison of Data Fitting with *DA* and *LF* Isotherms

Isotherm	SS_A	SS_D	SS_{SA}	SS_{SD}	SS_{total}
LF_{seq}	41.34	6.98	7.36	29.11	84.79
DA_{seq}	33.32	7.12	8.05	19.61	68.10
LF_{sim}	47.14	8.36	9.93	15.35	80.78
DA_{sim}	39.52	8.17	11.08	7.65	66.42

SS = sum of least squares multiplied by 10^4; *A* = primary adsorption; *D* = primary desorption; *SA* = secondary adsorption; *SD* = secondary desorption; seq = sequential regression; sim = simultaneous regression

$$K_j = \left(\frac{A_j}{B_j D_j}\right)^{1/n_D} \qquad a_{mj} = \frac{D_j}{\exp[-(K_j C_j)^{n_A}]} \tag{39}$$

where

$$A_j = a_{Aj} n_A K_A^{n_A} \left(\ln \frac{1}{x_j}\right)^{n_A - 1} (x_j - x^L) E_j \qquad B_j = n_D C_j^{n_D - 1}$$

$$C_j = \ln \frac{1}{x_j - x^L} \qquad D_j = a_{Aj} - a^L$$

The predictions of the secondary desorption isotherms are compared with the experimental data points, as shown in Figures 4 and 5. Figure 4 shows predictions using the LF isotherm for both primary and secondary processes, while Figure 5 shows those based on the DA isotherm. Fair agreement is seen for both predictions, although the DA-based procedure shows a slight advantage (see also Table 4). The average relative error for prediction of the secondary desorption curves using the proposed model with the DA isotherm was 2.9%, averaged over all data points.

Experimental data for the secondary adsorption isotherms are shown in Figures 6 and 7 and compared with theoretical predictions. Prediction of the secondary adsorption isotherms

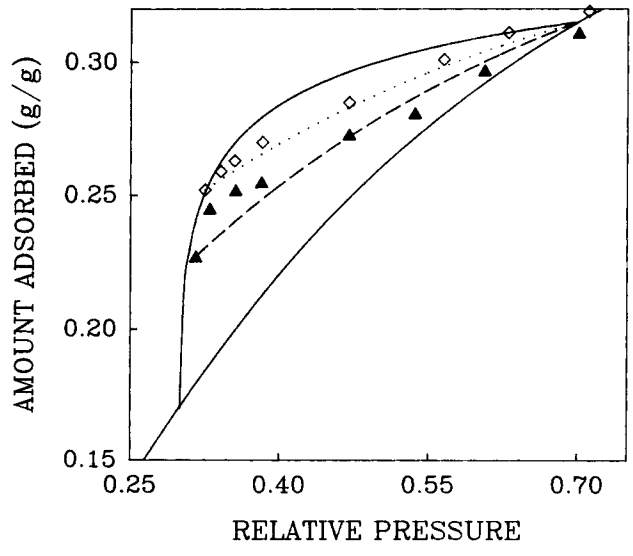

Figure 6. Experimental data on secondary adsorption (symbols) vs. theoretical predictions using the LF isotherm (curves).

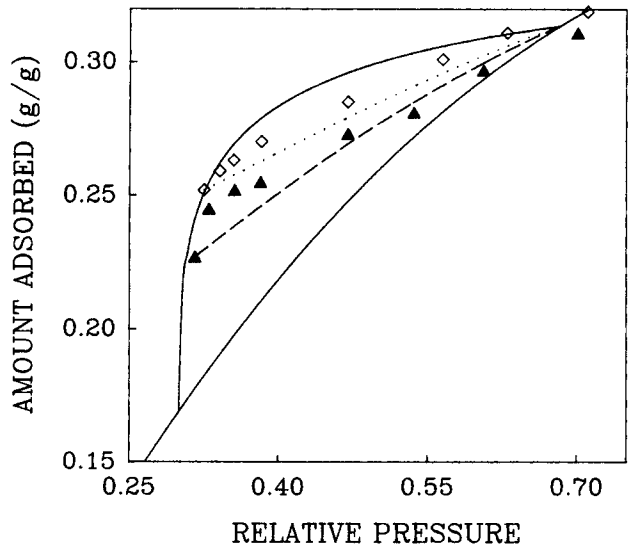

Figure 7. Same as in Figure 6, except for the DA isotherm.

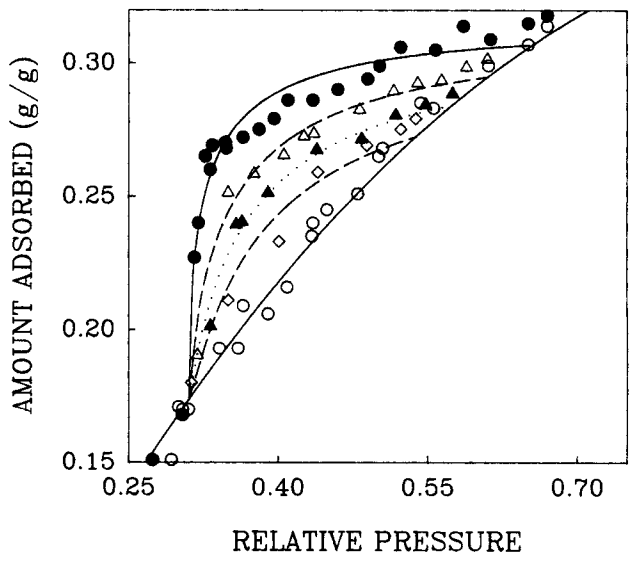

Figure 8. Simultaneous regression analysis of primary adsorption, and primary and secondary desorption data, using the DA isotherm, to yield parameters in Table 4.

is quite straightforward; Eq. 32 can be used in conjunction with the primary adsorption isotherm, Eq. 26 or 27, to calculate a_{SA} directly, starting from point i on the secondary desorption curve. Figures 6 and 7 differ only in the isotherm used for the primary adsorption: the LF isotherm is used for Figure 6 and DA for Figure 7. The average relative error for prediction of the secondary adsorption curves using the DA isotherm was 1.8%, averaged over all data points.

When experimental data on primary adsorption, and primary and secondary desorption are available, the model for secondary desorption proposed here can be used to evaluate all parameters a_{mA}, K_A, n_A, a_{mD}, K_D, n_D, x^L and x^U simultaneously by nonlinear regression. The parameters obtained in this manner are given in Table 5. These parameters may then be used for predicting secondary adsorption as well as further secondary desorption curves. The results for the simultaneous regression based on the DA isotherm are shown in Figure 8. The parameters obtained in this manner are better than those obtained from only primary adsorption and primary desorption data. Table 5, statistical analysis based on the simultaneous regression, shows that the DA isotherm yields better results.

Summary

Primary and secondary adsorption-desorption equilibrium data of water vapor on silica gel were measured at 25°C. The experimental results showed significant hysteresis loops in the range of relative pressure $P/P_o = 0.3$ to 0.7.

For the evaluation of experimental data, a simple method was proposed based on the network pore blocking theory of adsorption hysteresis. The main assumptions of the proposed method are:

- Capillary condensation phenomena controlled the sorption processes in the whole range of the hysteresis loop, and the secondary issues of surface adsorption in this domain was neglected.
- The empirical relationship $a' = a' - \kappa \ln (x^U/x)$ was used to represent decompression of the liquid phase and nucleation or vaporization from surface clusters in the whole hysteresis domain.
- The primary and secondary desorption curves could be described by the same mathematical form of isotherms.
- The secondary desorption isotherms could then be calculated using the ratio of the slopes of the secondary desorption and the primary adsorption at the onset of secondary desorption, being stipulated by the pore blocking theory.

A simple expression for this ratio was derived, which required neither connectivity nor size distribution functions. Only parameters of the primary adsorption and the primary desorption isotherms were needed for *a priori* computation of the secondary curves.

The proposed method was applied to the experimental sorption data of water vapor on silica gel. A sequential evaluation procedure was used to find the parameters of primary adsorption and primary desorption isotherms and the position of their intersections. The predicted secondary desorption and adsorption isotherms agreed well with the experimental data.

Table 5. Simultaneous Regression Analysis of Primary Adsorption, Primary Desorption, and Secondary Desorption Data

Isotherm	a_{mA}	K_A	n_A	a_{mD}	K_D	n_D	x^L	x^U	κ^*
LF	0.455	3.947	1.579	0.160	9.096	0.554	0.313	0.679	0.022
DA	0.356	0.690	1.555	0.137	0.189	2.259	0.311	0.655	0.014

*κ was calculated separately (see text).

Acknowledgment

This work was supported by the NSF under Grant CTS-9212279 and in part by the Donors to the Petroleum Research Fund, administered by the American Chemical Society.

Notation

a = amount adsorbed, g/g
a_m = parameter of isotherm
A = adsorption potential $= RT \ln (P_o/P)$
C = connectivity
E_o = characteristic energy
$f(r)$ = bond (window) radius distribution function
$g(r)$ = site (pore) radius distribution function
K = parameter of isotherm
n = parameter of isotherm
p = bond filling probability, Eq. 2
P = absolute pressure
P_o = saturation pressure
q = site filling probability, Eq. 3
R = gas constant
RRMSE = residual root mean square error
r = bond (window) or site (pore) radius
S = fraction of pores filled, defined by Eq. 7
SS = sum of least squares, Eq. 33
T = absolute temperature
u = probability that a bond is connected to the vapor during secondary desorption
v = probability that a bond is connected to the vapor during secondary adsorption
V = micropore volume
V_L = molar volume of liquid adsorbate
V_o = total micropore volume
x = relative pressure, P/P_o

Greek letters

β = affinity coefficient
κ = empirical constant
σ = interfacial tension

Subscripts

A = primary adsorption
cal = calculated
D = primary desorption
exp = experimental
i = ith secondary adsorption
j = jth secondary adsorption
SA = secondary adsorption
SD = secondary desorption

Superscripts

L = lower limiting (closure) point
r = real
t = theoretical
U = upper limiting (closure) point

Literature Cited

Baker, F. S., and K. S. W. Sing, "Specificity in the Adsorption of Nitrogen and Water on Hydroxylated and Dehydroxylated Silicas," *J. Colloid Interf. Sci.*, **55**, 605 (1976).

Baksh, M. S. A., "Development, Characterization, and Application of New Adsorbents for Separation by Adsorption," PhD Diss., State Univ. of New York at Buffalo (1991).

Ball, P. C., and R. Evans, "On the Mechanism for Hysteresis of Gas Adsorption on a Mesoporous Substrates," *Europhys. Lett.*, **4**, 715 (1987).

Ball, P. C., and R. Evans, "Temperature Dependence of Gas Adsorption on a Mesoporous Solid: Capillary Criticality and Hysteresis," *Langmuir*, **5**, 714 (1989).

Barrer, R. M., N. McKenzie, and J. S. S. Reay, "Capillary Condensation in Single Pores," *J. Colloid Sci.*, **11**, 479 (1956).

Broadbent, S. R., and J. M. Hammersley, "Percolation Processes: I. Crystals and Mazes," *Proc. Camb. Phil. Soc.*, **53**, 629 (1957).

Burgess, C. G. V., D. H. Everett, and S. Nuttal, "Adsorption Hysteresis in Porous Materials," *Pure Appl. Chem.*, **61**, 1845 (1989).

Everett, D. H., "Adsorption Hysteresis," *The Solid-gas Interface*, Vol. 2, E. A. Flood, ed., p. 1055, Marcel Dekker, New York (1967).

Everett, D. H., and J. M. Haynes, "Model Studies of Capillary Condensation: I. Cylindrical Pore Model with Zero Contact Angle," *J. Colloid Interf. Sci.*, **38**, 125 (1972).

Gregg, S. J., and K. S. W. Sing, *Adsorption Surface Area and Porosity*, 2nd ed., Academic Press, London (1982).

Jury, S. H., and H. R. Edwards, "The Silica Gel-Water Vapor Sorption Therm," *Can. J. Chem. Eng.*, **49**, 663 (1971).

Kapoor, A., J. A. Ritter, and R. T. Yang, "On the Dubinin-Radushkevich Equation for Adsorption in Microporous Solids in the Henry Law Region," *Langmuir*, **5**, 1118 (1989).

Katz, S. M., "Permanent Hysteresis in Physical Adsorption: A Theoretical Discussion," *J. Phys. Chem.*, **53**, 1166 (1949).

Kinnlburgh, D. G., "General Purpose Adsorption Isotherms," *Environ. Sci. Technol.*, **20**, 895 (1986).

Liu, H., L. Zhang, and N. A. Seaton, "Determination of the Connectivity from Nitrogen Sorption Measurements: II. Generalization," *Chem. Eng. Sci.*, to be published (1993).

Lunde, P. J., and F. L. Kester, "Chemical and Physical Gas Adsorption in Finite Multimolecular Layers," *Chem. Eng. Sci.*, **30**, 1497 (1975).

Mason, G. "The Effect of Pore Space Connectivity on the Hysteresis of Capillary Condensation in Adsorption-Desorption Isotherms," *J. Colloid Interf. Sci.*, **88**, 36 (1982).

Mason, G., "A Model of Adsorption-Desorption Hysteresis in which Hysteresis is Primarily Developed by the Interconnections in a Network of Pores," *Proc. R. Soc. Lond.*, **A390**, 47 (1983).

Mason, G., "Determination of the Pore-size Distribution and Pore-Space Interconnectivity of Vycor Porous Glass from Adsorption-Desorption Hysteresis Capillary Condensation Isotherms," *Proc. R. Soc. Lond.*, **A415**, 453 (1988).

Mikhail, R. S., S. Brunauer, and E. E. Bodor, "Investigations of a Complete Pore Structure Analysis: I. Analysis of Micropores," *J. Colloid Interf. Sci.*, **26**, 45 (1968).

Mikhail, R. S., and F. A. Shebl, "Adsorption in Relation to Pore Structure of Silicas: II. Water Vapor Adsorption on Wide-Pore and Microporous Silica Gels," *J. Colloid Interf. Sci.*, **34**, 65 (1970).

Naono, H., R. Fujiwara, and M. Yagi, "Determination of Physisorbed Waters on Silica Gel and Porous Silica Glass by Means of Desorption Isotherms of Water Vapor," *J. Colloid Interf. Sci.*, **76**, 74 (1980).

Neimark, A. V., "A Percolation Method for Calculating the Pore Size Distribution in Materials of Intermediate Porosity Based on the Adsorption and Desorption Isotherms in Hysteresis Region," *Russian J. Phys. Chem.*, **60**, 1045 (1986).

Neimark, A. V., "Percolation Theory of Capillary Hysteresis Phenomena and Its Application for Characterization of Porous Solids," *Characterization of Porous Solids II*, F. Rodriguez-Reinoso, J. Rouquerol and K. S. W. Sing, eds., p. 67, Elsevier, Amsterdam (1991).

Nonaka, A., and E. Ishizaki, "Stepwise Multilayer Adsorption of Water Vapor on Silica at Temperatures from 130 to 150°C," *J. Colloid Interf. Sci.*, **62**, 381 (1977).

Pan, D., and A. Mersmann, "Multilevel Adsorption and Hysteresis in Well-Defined Zeolite Sorbents," *Zeolites*, **10**, 210 (1990).

Park, I., and K. S. Knaebel, "Adsorption Breakthrough Behavior: Unusual Effects and Possible Causes," *AIChE J.*, **38**, 660 (1992).

Parlar, M., and Y. C. Yortsos, "Percolation Theory of Vapor Adsorption-Desorption Processes in Porous Materials," *J. Colloid Interf. Sci.*, **124**, 162 (1988).

Parlar, M., and Y. C. Yortsos, "Nucleation and Pore Geometry Effects in Capillary Desorption Processes in Porous Media," *J. Colloid Interf. Sci.*, **132**, 425 (1989).

Pendleton, P., and A. C. Zettlemoyer, "A Study of the Mechanism of Micropore Filling: II. Pore Filling of a Microporous Silica," *J. Colloid Interf. Sci.*, **98**, 439 (1984).

Rao, K. S., "Hysteresis in Sorption: III. Permanence and Scanning of the Hysteresis Loop. Silica Gel-Water System," *J. Phys. Chem.*, **45**, 513 (1941).

Ritter, J. A., and R. T. Yang, "Equilibrium Theory for Hysteresis-

Dependent Fixed-Bed Desorption," *Chem. Eng. Sci.*, **46**, 563 (1991).
Rudisill, E. N., J. J. Hacskaylo, and M. D. LeVan, "Coadsorption of Hydrocarbons and Water on BPL Activated Carbon," *Ind. Eng. Chem. Res.*, **31**, 1122 (1992).
Seaton, N. A., "Determination of the Connectivity of Porous Solids from Nitrogen Sorption Measurements," *Chem. Eng. Sci.*, **46**, 1895 (1991).
Sing, K. S. W., "Characterization of Porous Solids: An Introductory Survey," *Characterization of Porous Solids II*, F. Rodriguez-Reinoso, J. Rouquerol, and K. S. W. Sing, eds., p. 1, Elsevier, Amsterdam (1991).
Sing, K. S. W., and J. D. Madeley, "The Surface Properties of Silica Gels. II. Adsorption of Water Vapour," *J. Appl. Chem.*, **4**, 365 (1954).
Someshwar, A. V., and D. L. Peshori, "Corona Discharge Effects in Gas-Solid Adsorption: Water Vapor on Silica Gel and Fly Ash," *Chem. Eng. Commun.*, **50**, 331 (1987).
Stoeckli, H. F., "A Generalization of the DR Equation for the Fitting of Heterogeneous Micropore Systems," *J. Coll. Interf. Sci.*, **59**, 184 (1977).
Van den Bulck, E., "Isotherm Correlation for Water Vapor on Regular-Density Silica Gel," *Chem. Eng. Sci.*, **45**, 1425 (1990).
van Bemmelen, J. M., "Die Adsorption. Das Wasser in den Kolloiden, besonders in dem Gel der Kieslsaure," *Z. Annorg. Allgem. Chem.*, **13**, 231 (1897).
Wall, G. C., and J. C. Brown, "The Determination of Pore-Size Distributions from Sorption Isotherms and Mercury Penetration in Interconnected Pores: The Application of Percolation Theory," *J. Colloid Interf. Sci.*, **85**, 141 (1981).
Yang, R. T., *Gas Separation by Adsorption Processes*, Butterworth, Boston (1987).
Yanuka, M., "The Mixed Bond-Site Percolation Problem and Its Application to Capillary Phenomena in Porous Media," *J. Colloid Interf. Sci.*, **134**, 198 (1990).
Zhdanov, V. P., V. B. Fenelonov, and D. K. Efremov, "Determination of Pore-Size Distribution from Sorption Isotherms: Application of Percolation Theory," *J. Colloid Interf. Sci.*, **120**, 218 (1987).

Manuscript received Aug. 4, 1992, and revision received Oct. 16, 1992.